MNDO Analysis of Regiospecificity in Reactions of 1,5- and 2,5-Substituted Tetrazoles

B. Vernon Cheney

The Upjohn Company, Kalamazoo, Michigan 49007-4940

MNDO calculations have provided useful insights for analysis of both the metalation and alkylation steps of the reactions of 1,5- and 2,5-substituted tetrazoles with *tert*-butyllithium and iodomethane. Although the results suggest that equilibrium thermodynamics will favor the formation of the 1,5- and 2,5-diethyl compounds, the relative height of the calculated energy barriers indicates that kinetics will favor production of the 5-(2-propyl) product in both cases. Factors affecting the ultimate balance in favor of the thermodynamic product in the case of 2-methyl-5-ethyltetrazole and the kinetic product in the case of 1-methyl-5-ethyltetrazole are revealed in the details of the calculations. Since the models employed are appropriate only for a medium of unit dielectric constant, solvent effects on the rates of reaction have been examined by means of Laidler–Eyring theory, which is useful in systems where many of the molecules exhibit large dipole moments.

Introduction

As part of a synthetic program designed to produce a variety of substituted tetrazoles, Thomas and Cudahy[1] carried out two reactions that proceeded according to the following scheme:
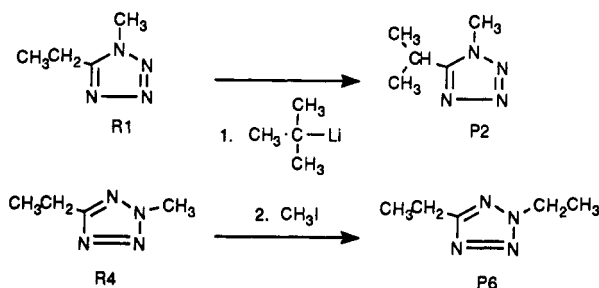
When 1-methyl-5-ethyltetrazole (**R1**) was treated with *tert*-butyllithium (**R2**) in THF followed by addition of CH₃I (**R3**), alkylation occurred only on the ethyl substituent giving 1-methyl-5-(2-propyl)tetrazole (**P2**) in low yield as the exclusive product. On the other hand, use of 2-methyl-5-ethyltetrazole (**R4**) as starting material led to alkylation at the methyl group yielding 2,5-diethyltetrazole (**P6**) in moderate quantity. The lack of 1,5-diethyltetrazole (**P3**) and 2-methyl-5-(2-propyl)tetrazole (**P5**) in the respective reaction mixtures seems quite puzzling. Since the regiospecificity holds for many 1,5- and 2,5-substituted tetrazoles,[1-3] as well as several electrophiles other than CH₃I, theoretical investigation of the phenomenon appears worthwhile.

As a means of gaining some understanding of the factors affecting regiospecificity, a series of MNDO[4] calculations have been performed on the molecules involved in these reactions. Semiempirical molecular orbital calculations have provided useful insights into many chemical re-

actions[4-9] that are impractical to consider with ab initio techniques. Although the MNDO procedure exaggerates reaction barriers, the results generally may be used in a qualitative sense to compare features of different mechanistic pathways and to investigate the nature of structures corresponding to stationary points on the potential surface.[4-8]

In this study, reaction at both the methyl and ethyl substituents is examined by searching the MNDO potential surfaces corresponding to the metalation and alkylation steps. Relative stabilities of transition-state complexes, reactants, intermediates, and products are assessed from calculated values of the heat of formation, H_f. The favored kinetic pathways are determined by comparison of the calculated energy barriers, ΔE^*, for attack at each site.

Theory

The reactions under consideration in this study are bimolecular processes that may be represented by the expression

$$A + B \rightleftharpoons M^* \rightleftharpoons X + Y \qquad (1)$$
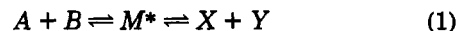
where A and B are reactants, M^* is the transition-state complex, and the products are X and Y. The rate constant, k_0, for the forward reaction of eq 1 taking place in a medium of unit dielectric constant may be calculated from transition-state theory[10] by means of eq 2 where k is Boltz-

$$k_0 = \frac{kT}{h} \frac{q_{M^*} V}{q_A q_B v_f} \exp(-\Delta E^*/RT) \qquad (2)$$

mann's constant; T is the absolute temperature; h is Planck's constant; q_A, q_B, and q_{M^*} are the partition functions for reactants and the transition-state complex; V is approximately the molar volume of the solvent; v_f is

---

[•] Abstract published in *Advance ACS Abstracts,* February 15, 1994.

(1) Thomas, E. W.; Cudahy, M. M. *J. Org. Chem.* **1993,** *58,* 1623.

(2) Moody, C. J.; Rees, C. W.; Young, R. G. *J. Chem. Soc. Perkin Trans. 1* **1991,** 323.

(3) Quast, H.; Bieber, L.; Meichsner, G.; Regnat, D. *Chem. Ber.* **1988,** *121,* 1285.

(4) Dewar, M. J. S.; Thiel, W. *J. J. Am. Chem. Soc.* **1977,** *99,* 4899, 4907.

(5) Carrion, F.; Dewar, M. J. S. *J. Am. Chem. Soc.* **1984,** *106,* 3531.

(6) Hrusak, J. *Org. Mass Spectrosc.* **1990,** *25,* 503.

(7) Hrusak, J. *Theor. Chim. Acta* **1990,** *78,* 203.

(8) Suner, G. A.; Deya, P. M.; Saa, J. M. *J. Am. Chem. Soc.* **1990,** *112,* 1467.

(9) Dewar, M. J. S.; Yuan, Y.-C. *J. Am. Chem. Soc.* **1990,** *112,* 2088, 2095.

(10) Frost, A. A.; Pearson, R. G. *Kinetics and Mechanism,* 2nd ed.; John Wiley & Sons, Inc.: New York, 1961; Chapters 5 and 7.

the free volume in the condensed medium;[11] and R is the gas constant per mole. However, if this is done, the well-known failing of MNDO in exaggerating energy barriers becomes evident from the extremely small values of the calculated rates compared to experiment. Nevertheless, differences in the barriers for competing processes provide useful information as to which one is kinetically favored.

Since several of the species in the reactions under study exhibit large dipole moments, electrostatic contributions to the free energy of solvation may play a major role in determining the outcome of the reactions. This effect may be treated qualitatively in terms of the Kirkwood[12] expression for the change of free energy, ΔG_s, involved in the transfer of a strong dipole of moment μ from a vacuum into a cavity of radius r in a continuous medium of dielectric constant D:

$$\Delta G_s = -\frac{\mu^2}{r^3}\left[\frac{D-1}{2D+1}\right] \qquad (3)$$

Although r depends upon the size of the molecule, it is not well defined for nonspherical systems. To make estimates of ΔG_s in this work, the radius of the solvent cavity is taken as

$$r = \max(d_1 + \rho_1, ..., d_n + \rho_n) \qquad (4)$$

where d_i is the distance from the center of mass to atom i and ρ_i is the van der Waals' radius of the atom.

By using eq 3 to consider solvation of the reactants, Laidler and Eyring[13] obtained the following relationship for the effect of solvent on the rate constant k:

$$\ln k = \ln k_0 - \frac{N}{RT}\frac{(D-1)}{(2D+1)}\left[\frac{\mu_A^2}{r_A^3} + \frac{\mu_B^2}{r_B^3} - \frac{\mu_{M*}^2}{r_{M*}^3}\right] \qquad (5)$$

In this expression, N is Avogadro's number. The approximate nature of eq 5 permits only crude estimates of solvent-induced rate changes, but useful qualitative comparisons may be made of the effect on competing processes which involve reactants and transition-state complexes with significant differences in size and dipole moment.

For a pair of competing reactions, where A_1 and A_2 represent either isomers or a single molecule with two different sites of attack for reagent B, the following expression may be obtained from eqs 2 and 5 for the relative magnitude of the rate constants, k_1 and k_2:

$$\ln\frac{k_1}{k_2} \approx \frac{\Delta E_2^* - \Delta E_1^*}{RT} + \beta_2^* - \beta_1^* \qquad (6)$$

where the solvent contribution to $\ln k_i$ from eq 5 is denoted as β_i^*. The preexponential factors from eq 2 cancel in the derivation of eq 6 since the partition functions for isomers A_1 and A_2 are nearly equal, as are those for the transition-state complexes, M_1^* and M_2^*. Equation 6 demonstrates that the reaction rates differ in this case as a result of differences in the energy barriers and in the solvent effects. Furthermore, this comparison eliminates some of the error due to bias of the MNDO and Kirkwood models.

While lithium–hydrogen exchange reactions are generally reversible, alkylation of organolithium compounds

with alkyl iodides usually favors product formation.[14] To avoid unwarranted assumptions regarding reversibility in the cases under study, eq 6 has been applied to both the forward and backward reactions of the metalation and alkylation steps.

Computational Methods

MNDO calculations were performed with the MOPAC 6.0 computer program.[15] Single molecules were treated at the restricted Hartree–Fock level, and a limited HOMO-LUMO CI was employed to explore the singlet ground-state potential surface of each molecular complex. During preliminary searches, one or two coordinates were fixed at different values as the reactants were brought into proximity in order to find the probable location of stationary points. However, in the final computations, all geometric parameters were optimized. Stationary points were characterized by diagonalizing the calculated Hessian matrix and checking the number of negative eigenvalues.[16]

The barrier height for the forward reaction in eq 1 is given by eq 7, and the Laidler–Eyring solvation factors for

$$\Delta E^* = H_f(M^*) - H_f(A) - H_f(B) \qquad (7)$$

THF are calculated from eq 8, where $T = 293$ K and D_{THF}

$$\beta_i^* = 230.7\left[\frac{\mu_A^2}{r_A^3} + \frac{\mu_B^2}{r_B^3} - \frac{\mu_{M*}^2}{r_{M*}^3}\right] \qquad (8)$$

$= 7.58$. Equivalent expressions for ΔE^* and β_i^* may be written for the backward reaction of eq 1 in terms of the calculated values of H_f, μ, and r for M*, X, and Y.

The magnitude of β_i^* is undoubtedly overestimated when small, highly polar molecules such as *tert*-butyllithium and lithium iodide are involved in the reaction. A molecule of this type is likely to interact strongly with its polar neighbors to form a stable complex where μ is smaller and r is greater than the values for the molecule alone. Nevertheless, the large magnitude of β_i^* indicates that the environment of the molecule markedly affects reactivity, and the sign of the term reveals the direction of the effect. Furthermore, the relative effects of solvation on competing processes may be revealed by differences in the estimates of β_i^* used in this work.

Results and Discussion

Reaction Models. The molecules and complexes considered in the reaction pathways for tetrazoles **R1** and **R4** are illustrated in Schemes 1 and 2, respectively. In the initial series of calculations on these structures, optimized geometries were found for reactants (**R1–R4**), the metalated intermediates (**I1–I4**), and the expected final products (**P1–P6**) of the two reactions. Values of H_f, μ and r obtained from these calculations are reported in Table 1.

If a steady state in the concentration of the lithiated intermediate I_i is achieved at the final temperature of the system (*i.e.*, $d[I_i]/dt = 0$), the rate at which product P_i is formed from reactant **R** will be given by

(11) Kincaid, J. F.; Eyring, H.; Stearn, A. E. *Chem. Rev.* 1941, 3, 301.
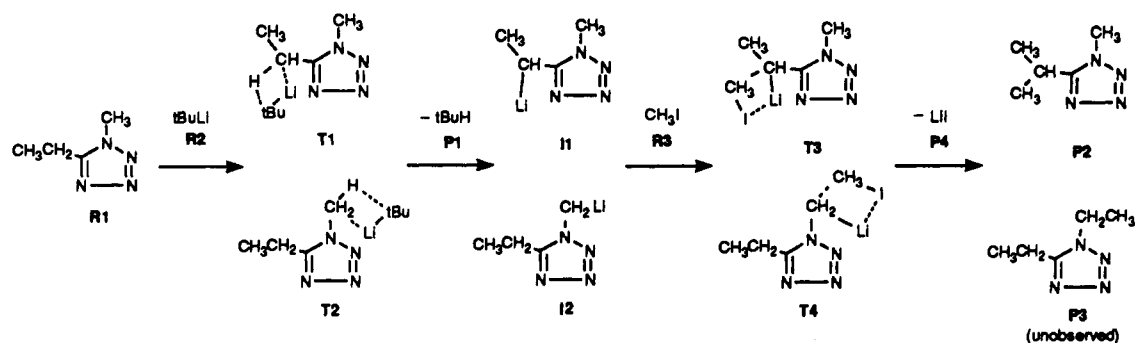(12) Kirkwood, J. G. *J. Chem. Phys.* 1934, 2, 351.
(13) Laidler, K. J.; Eyring, H. *Ann. N. Y. Acad. Sci.* 1940, 39, 303.

(14) Powell, P. *Principles of Organometallic Chemistry*, 2nd ed.; Chapman & Hall: London, 1988; pp 39–41.
(15) Stewart, J. J. P. *J. Comput.-Aided Mol. Des.* 1990, 4, 1.
(16) McIver, J. W.; Kormornicki, A. *J. Am. Chem. Soc.* 1972, 94, 2625.
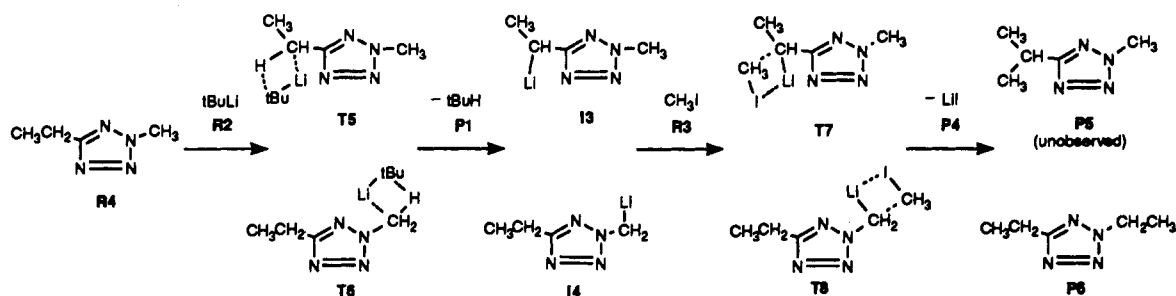
Scheme 1

Scheme 2

Table 1. Calculated Heat of Formation (H_f), Dipole Moment (μ), and Radius (r) of the Solvent Cavity for the Optimized Structure of Each Reactant, Intermediate, and Product

molecule	H_f kcal/mol	μ, D	r,[a] Å
R1: 1-methyl-5-ethyl-1H-tetrazole	33.7	5.5	4.9
R2: tert-butyllithium	-25.2	6.1	3.7
I1: 1-methyl-5-(1-lithioethyl)-1H-tetrazole	21.5	4.0	4.8
I2: 1-(lithiomethyl)-5-ethyl-1H-tetrazole	27.3	2.4	5.1
P1: 2-methylpropane	-26.8	0.0	3.3
R3: iodomethane	2.2	1.4	3.5
P2: 1-methyl-5-(2-propyl)-1H-tetrazole	32.1	5.6	4.7
P3: 1,5-diethyl-1H-tetrazole	29.0	5.5	5.1
P4: lithium iodide	-2.0	7.8	4.0
R4: 2-methyl-5-ethyl-2H-tetrazole	35.3	2.3	5.2
I3: 2-methyl-5-(1-lithioethyl)-2H-tetrazole	30.2	3.3	5.1
I4: 2-(lithiomethyl)-5-ethyl-2H-tetrazole	31.2	6.9	5.2
P5: 2-methyl-5-isopropyl-2H-tetrazole	33.7	2.2	4.9
P6: 2,5-diethyl-2H-tetrazole	29.4	2.4	5.6

[a] See eq 4 for definition of r.

$$\frac{d[P_i]}{dt} = \frac{k_{mi}k_{ai}[R][tBuLi] - k_{-mi}k_{-ai}[tBuH][LiI][P_i]}{k_{-mi}[tBuH] + k_{ai}[CH_3I]} \quad (9)$$

where index i differentiates the reaction sites in R, k_{mi} and k_{ai} are the forward rate constants for the metalation and alkylation steps, and k_{-mi} and k_{-ai} are the rate constants for the reverse reactions. At equilibrium, where $d[P_i]/dt = 0$, the calculated concentration ratio of product isomers in the 1,5-substituted case is

$$\frac{[P2]}{[P3]} = \exp[[H_f(P3) - H_f(P2)]/RT] \quad (10)$$

A similar expression may be given in terms of P5 and P6 for the 2,5-substituted case. The calculated values of the ratios are [P2]/[P3] = 0.005 and [P5]/[P6] = 0.0007. In both reactions, the 5-(2-propyl) product is predicted to be highly disfavored from a thermodynamic standpoint. Unavoidable steric interactions between the substituent methyl groups and the tetrazole ring serves to destabilize

Table 2. Calculated Heat of Formation (H_f), Dipole Moment (μ), and Radius (r) of the Solvent Cavity for the Transition-State Complexes

complex	molecules	product substituents	H_f kcal/mol	μ, D	r,[a] Å
T1	R1 + R2	1-methyl-5-(lithioethyl)	21.6	2.8	5.6
T2	R1 + R2	1-(lithiomethyl)-5-ethyl	29.2	2.4	6.0
T3	I1 + R3	1-methyl-5-(2-propyl)	78.9	6.3	6.6
T4	I2 + R3	1,5-diethyl	87.4	2.5	7.5
T5	R4 + R2	2-methyl-5-(lithioethyl)	27.5	3.7	6.0
T6	R4 + R2	2-(lithiomethyl)-5-ethyl	32.2	4.3	6.5
T7	I3 + R3	2-methyl-5-(2-propyl)	85.1	6.8	7.2
T8	I4 + R3	2,5-diethyl	90.5	4.1	7.3

[a] See eq 4 for definition of r.

5-(2-propyl) isomer relative to the less crowded 5-ethyl isomer. Although the small value of [P5]/[P6] is in accord with observation, the value of [P2]/[P3] is seriously at odds with experimental findings. This evidence indicates that kinetic factors underlie the lack of P3 as a reaction product of the 1,5-substituted tetrazole.

Factors Affecting Reaction Kinetics. To obtain estimates of the energy barriers, a second series of calculations was carried out to locate transition states for the metalation and alkylation steps of each reaction. Searches for stationary points on the potential surfaces of the systems led to complexes T1-T8. Although the distance between substituents in the 2,5-substituted tetrazole R4 appears to open up two avenues of approach for tert-butyllithium at each site, preliminary calculations revealed that the approaches found in T5-T8 are clearly preferred. Relaxation following slight perturbations of the transition-state structures led to stable reactant and product complexes in all cases.

Values of H_f, μ, and r for the transition-state complexes are given in Table 2, and the structures are portrayed in Figures 1-3. No illustrations for T5 and T7 are shown since reaction at the ethyl substituent of R4 yields complexes where the critical features resemble those of T1 and T3 in Figure 1.

As shown in Tables 1 and 2, the dipole moments for the various molecules and complexes vary from 0 to 7.8 D. Of
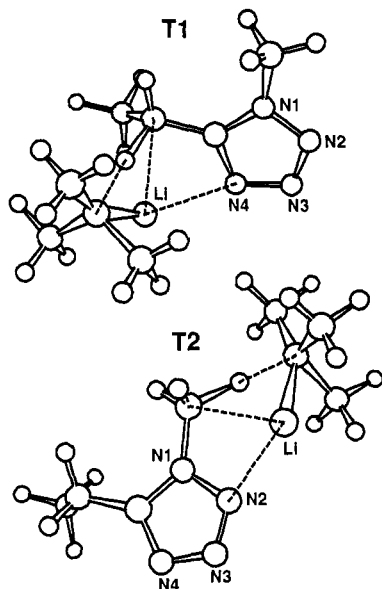
Figure 1. Transition-state complexes in the metalation pathway of **R1**. Dashed lines indicate close approach of key atoms in the two reactants. Transfer of the lithium cation to the tetrazole substituent is aided by a significant attractive interaction with the nearest ring nitrogen atom, NX. A hydrogen atom, HX, carrying a significant positive charge is shifted simultaneously from the substituent carbon, CX, to the tertiary carbon, CB, of **R2**. The Li$\cdots$NX, Li$\cdots$CX, and C$B\cdots$HX distances are quite similar in the two structures; the respective values, within ± 0.02 Å, are 2.24, 2.31, and 1.54 Å. Average bond distances CX–HX and CB–Li involving the atoms undergoing transfer are, respectively, 1.41 and 2.11 Å.
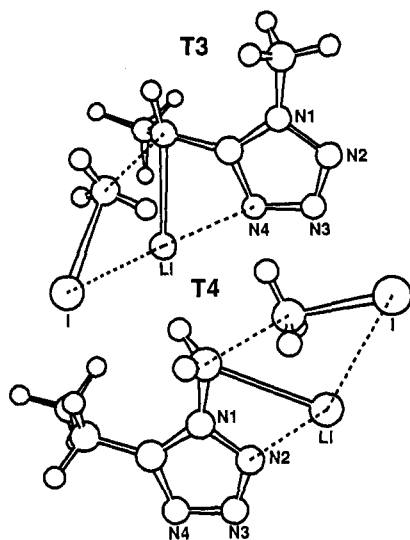

Figure 2. Transition-state complexes in the alkylation pathway of **R1**. **T3** is produced from the metalated intermediate **I1**, and **T4** is generated from **I2**. In this reaction, the products are formed upon transfer of the methyl group (CM) in **R3** to the tetrazole substituent. Corresponding distances between the key atoms marked by dashed lines differ by less than ± 0.03 Å in the two structures; the average values of the Li$\cdots$NX, Li$\cdots$I, and C$X\cdots$CM distances are 2.15, 2.92, and 2.08 Å, respectively. The CX–Li and CM–I bond distances in **T3** are 2.48 and 2.39 Å, respectively, while the values in **T4** are 2.81 and 2.28 Å.

particular note are the marked differences in μ exhibited by each pair of lithiated intermediates (**I1** vs **I2**, and **I3** vs **I4**) expected from competition of the alkyl substituents for the *tert*-butyllithium reagent. In a polarizable solvent, these differences will have a significant effect on the
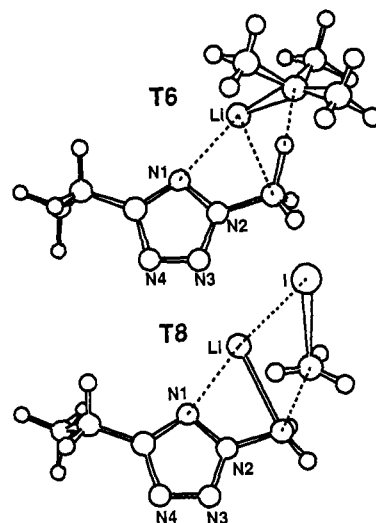

Figure 3. Transition-state complexes for metalation, **T6**, and for alkylation, **T8**, of the methyl substituent in **R4**. In **T6**, the Li$\cdots$N1, Li$\cdots$C2, and C$B\cdots$H2 distances, marked by dashed lines, are 2.13, 2.25, and 1.52 Å, respectively. The C2–H2 and CB–Li bonds are stretched to 1.42 and 2.10 Å. In **T8**, the Li$\cdots$N1, Li$\cdots$I, and C2$\cdots$CM distances are 2.19, 2.92, and 2.06 Å, respectively. The C2–Li and CM–I bond lengths are 2.45 and 2.34 Å.

approach to equilibrium for both the metalation and alkylation steps of the reaction. The transition-state complexes for competing alkylation reactions (**T3** vs **T4**, and **T7** vs **T8**) also exhibit large differences in dipole moment, and this plays an important role in determining the relative rates of methyl–lithium exchange in THF.

Underlying the calculated differences in μ are variations in the charge distributions of the various molecular structures. Lithium has a large positive charge in all molecules of which it is a component in these reaction systems. In the tetrazole ring, the nitrogen atoms next to C5 (N1 and N4) exhibit significant negative partial charges in every case, while N3 is nearly neutral. N2 carries a very small charge in the structures on the pathway for production of **P2**. However, polarization by Li$^{+\delta}$ induces a sizable negative charge on N2 in the complexes and intermediates found along the pathway to **P3**. The tetrazole substituent carbon under attack develops a significant negative charge in the metalation step, and the leaving hydrogen becomes more positive. The tertiary carbon in *tert*-butyllithium experiences a reduction of negative charge as **R2** moves from isolation into the transition-state complex. In the alkylation step, the charge on I is slightly positive in iodomethane, but develops to a significant negative value in the transition-state complex. At the same time, the methyl carbon in **R3** loses electronic population to become slightly positive.

Reaction Barriers. The reaction pathways are illustrated schematically in Figures 4 and 5. Whether **R1** or **R4** is used as starting material, the large difference in the height of the barriers for reverse metalation and forward alkylation of **I**$_i$ demonstrates that $k_{-mi} \gg k_{ai}$. In this case, eq 9 becomes

$$\frac{d[P_i]}{dt} \approx \frac{k_{mi}k_{ai}[\mathbf{R}][\text{tBuLi}]}{k_{-mi}[\text{tBuH}]} - k_{-ai}[\text{LiI}][\mathbf{P}_i] \quad (11)$$

In a system not yet at equilibrium, the production of isomer **P**$_1$ will be favored over **P**$_2$ if $k_{m1}k_{a1}/k_{-m1} > k_{m2}k_{a2}/k_{-m2}$ and $k_{-a1} < k_{-a2}$. The magnitude of k_{-ai} plays an important role
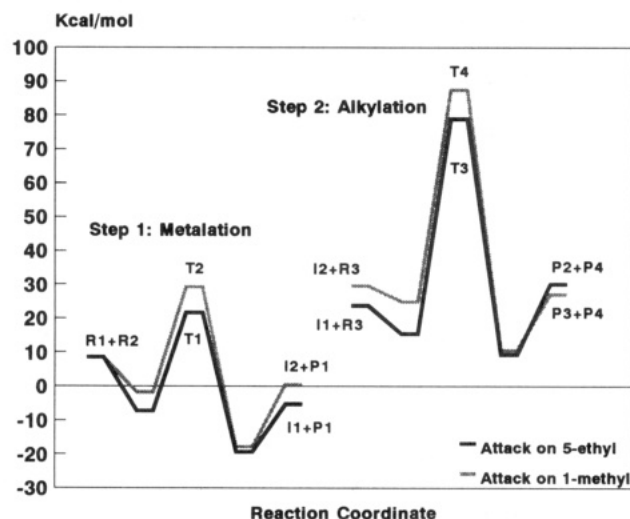
Figure 4. Stationary points on the potential surfaces for reactions using **R1** as starting material.
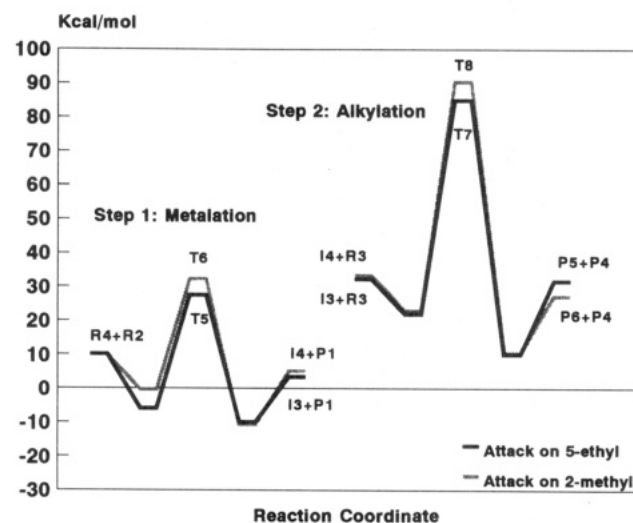

Figure 5. Stationary points on the potential surfaces for processes with **R4** as the starting reactant.

in determining how quickly the system comes to equilibrium and how much product is ultimately formed. Since the methods used in this study do not permit estimation of absolute rate constants, the discussion to follow in this section will focus on qualitative assessment of the kinetics through comparison of barrier heights. Electronic factors affecting the size of the barriers will also be considered.

In the metalation step of the 1,5-substituted tetrazole, reaction is favored at the 5-ethyl group at all points along the pathway. The calculated barrier for **T1** is about 8 kcal/mol lower than the one for **T2**. Stabilization of **T1** results from a strong $Li^{+\delta}-N4^{-\delta}$ electrostatic interaction. Similar energy-lowering electrostatic interactions have been noted in ab initio SCF calculations on lithiated *N*-methylformamide.[17] Since N2 carries a significantly smaller negative charge in **T2** than N4 does in **T1**, the $Li^{+\delta}-NX^{-\delta}$ interaction does not stabilize **T2** as effectively as **T1**. Furthermore, the stability of **I1** leads to a barrier for the reverse reaction at the 5-lithioethyl substituent that exceeds the forward barrier by almost 14 kcal/mol. In comparison, the barrier for the reverse reaction at the 1-lithiomethyl substituent of **I2** is only about 8 kcal/mol

(17) Bartolotti, L. J.; Gawley, R. E. *J. Org. Chem.* **1989**, *54*, 2980.

higher than the forward barrier. Although metalation of both substituents is predicted to be favorable, the evidence shows that reaction will occur much faster at the 5-ethyl substituent of **R1** and will be virtually irreversible. Therefore, **I1** is predicted to constitute the only pool of reactant available for methyl–lithium exchange upon addition of CH_3I.

In the alkylation step, reaction of the 5-(lithioethyl)-tetrazole is favored over the 1-(lithiomethyl)tetrazole at each stage in the pathway except the breakup of the product complex. **T3** is about 3 kcal/mol more stable than **T4**. The calculated barriers for methylation are much higher than those for metalation, indicating that this is the rate-controlling step of the reaction. In both **T3** and **T4**, the CX–Li bond of the metalated intermediate is completely dissociated in the complex, although the Li–I bond has not yet formed. Since the experimental heat of formation for lithium iodide is 14 kcal/mol lower than the value found in the MNDO calculation, the extremely high barriers in the alkylation reaction may be due in part to error in the calculated Li–I interaction. Nevertheless, the nearby negatively charged nitrogen atom eases removal of Li from the bonded carbon, as was found in the metalation step; and the relative height of the barriers for **T3** and **T4** may be ascribed to differences in the $Li^{+\delta}-NX^{-\delta}$ electrostatic interactions. Since the barrier to the reverse methyl–lithium exchange reaction at the 5-substituent is calculated to be about 6 kcal/mol lower than the one for the forward reaction, the net reaction does not favor product formation, and this accounts in part for the overall low yield of 1-methyl-5-(2-propyl)tetrazole. Although the reverse barrier to methyl–lithium exchange at the 1-substituent is approximately 3 kcal/mol higher than the forward barrier, the evidence from the calculations indicates that lack of **I2** in the reaction mixture will prevent formation of measurable quantities of the thermodynamically-favored 1,5-diethyl product until the system nears equilibrium.

Comparison of ΔE^* values obtained from reactions of the 2,5-substituted tetrazole reveals similar trends to those found for metalation and alkylation of the 1,5-substituted compound. However, in the metalation step, smaller differences are found between barriers to reaction at the two substituents, as well as between the forward and reverse barriers at either reaction site. In the alkylation step, the reverse barrier is higher than the forward barrier for both of the lithiated intermediates, indicating a balance toward product formation in either case. Although the calculations indicate that kinetic factors favor reaction at the 5-ethyl substituent in a medium with $D = 1$, the preference is clearly not as strong as in the case of the 1,5-substituted tetrazole.

Solvent Effects. Since $\beta_i^* \geq 0$ for all reactions considered in this study, most of the rates of reaction in THF are predicted by eq 5 to be slower than in a solvent with $D \approx 1$. However, it is the differing effects on competing reactions that are of interest in ascertaining the reasons for the observed regioselectivity in the tetrazole systems. Equation 6 provides a means of assessing solvent effects on the relative rates of competing reactions. Calculated values of the terms in eq 6 for the competitive systems under study are listed in Table 3. Since the MNDO method and the Kirkwood solvation model yield exaggerated energy differences, the findings in Table 3

Table 3. Calculated Effect of Differences in Energy Barriers and Free-Energy of Solvation on the Relative Magnitudes of Rate Constants for Competing Reactions

reaction 1 (at 5-ethyl)	reaction 2 (at 1- or 2-methyl)	$(\Delta E_2{}^* - \Delta E_1{}^*)/RT$	$\beta_2{}^* - \beta_1{}^*$	$\ln(k_1/k_2)$
R1 + R2 → I1 + P1	R1 + R2 → I2 + P1	12.7	5	17.7
I1 + P1 → R1 + R2	I2 + P1 → R1 + R2	3.0	−19	−16.0
I1 + R3 → P2 + P4	I2 + R3 → P3 + P4	4.5	5	9.5
P2 + P4 → I1 + R3	P3 + P4 → I2 + R3	19.3	11	30.3
R4 + R2 → I3 + P1	R4 + R2 → I4 + P1	7.8	−1	6.8
I3 + P1 → R4 + R2	I4 + P1 → R4 + R2	6.2	59	65.2
I3 + R3 → P5 + P4	I4 + R3 → P6 + P4	7.3	79	86.3
P5 + P4 → I3 + R3	P6 + P4 → I4 + R3	16.2	17	33.2

are useful only for qualitative comparisons of the effects, and this will be the emphasis of the discussion in this section.

In the 1,5-substituted case, the rate of metalation at the 5-position is predicted to be much faster than at the 1-position since the solvent effect $(\beta_2{}^* - \beta_1{}^* = 5)$ reinforces the effect due to the large difference in barriers. However, the reverse reactions are affected oppositely, and to a greater extent, as indicated by the difference $\beta_2{}^* - \beta_1{}^* = -19$. In this case a polarizable solvent is predicted to selectively promote the formation and repress the loss back to R1 of intermediate I1 over I2. The difference $\beta_2{}^* - \beta_1{}^* = 5$ calculated from the alkylation step reveals that THF favors formation of P2 over P3. On the other hand, $\beta_2{}^* - \beta_1{}^* = 11$ for reverse alkylation, so that THF will also increase the loss of P2 back to intermediate over P3. Nevertheless, since $\beta_i{}^* > 250$ for both reverse-alkylation reactions, a polarizable solvent will greatly reduce the rate of product loss back to the intermediate according to eq 5. This helps to compensate for the unfavorable equilibrium caused by the difference in the forward and reverse barriers to methylation at the 5-position. In any event, the calculations predict that a solvent with a high dielectric constant will have the effect of reinforcing the observed regiospecificity in the reaction of the 1,5-substituted tetrazole.

In the case of the 2,5-substituted tetrazole, the values of $(\Delta E_2{}^* - \Delta E_1{}^*)/RT$ for both the metalation and alkylation steps indicate that P5 will be formed at a much faster rate than the observed P6 in a medium of unit dielectric constant. Therefore, the calculations predict that P6 will predominate in such a medium only if the overall reaction achieves equilibrium. It is worthwhile to examine the effects of THF on the reaction rates of this system to determine whether the experimental results can be explained without assuming equilibrium.

Since $\beta_2{}^* - \beta_1{}^* = -1$, THF has a relatively minor effect on the relative rate of metalation at the 2-methyl and 5-ethyl positions. However, loss of intermediate I3 back to reactant will be greatly increased relative to I4 as a consequence of the solvent effect on the reverse metalation step, where $\beta_2{}^* - \beta_1{}^* = 59$. The magnitude of this difference suggests that solvent stabilization will cause I4 to predominate as the product in THF if metalation goes to completion. According to the data in Table 3, THF favors both the formation of P5 and its loss back to intermediate over the corresponding reactions involving P6. However, due to the stabilization of LiI in the polarizable medium, $\beta_i{}^* \geq 200$ for the reverse-alkylation reactions involving P5 and P6, and the principle effect of THF is a marked reduction in the rate of product loss back to intermediate compared to a medium with $D = 1$. However, if 2-(lithio-methyl)-5-ethyltetrazole (I4) does constitute the major pool of intermediate available for the alkylation step, the final product will be the observed 2,5-diethyltetrazole

whether methyl–lithium exchange goes to completion or not. Since the calculated barriers to metalation are much lower than the barriers to alkylation and THF slows the approach to equilibrium, it is likely that the lithium–hydrogen exchange reaction does go to completion, while methyl–lithium exchange does not within the time allowed for the reaction by Thomas and Cudahy.

Conclusion

Reaction of 1-methyl-5-ethyltetrazole with *tert*-butyllithium and iodomethane in THF leads to only one product, 1-methyl-5-(2-propyl)tetrazole. On the other hand, use of 2-methyl-5-ethyltetrazole as starting material yields only 2,5-diethyltetrazole. To discern the factors underlying the regiospecificity of these reactions, a series of MNDO calculations has been undertaken to investigate alternative mechanisms. At equilibrium in a medium with a unit dielectric constant, the calculations predict that the 1,5- and 2,5-diethyltetrazoles should be the dominant products. By locating transition states on the potential energy surfaces of the systems, estimates have been made of the energy barriers that affect reaction kinetics. Although quantitative accuracy in the barriers is not obtained with this approximate semiempirical technique, the calculations reveal important electronic factors affecting the mechanism, and qualitative differences in the barrier heights aid in providing a rationale for the experimental findings.

Lack of the favored thermodynamic product in the reaction of the 1,5-substituted tetrazole indicates that kinetic factors determine the outcome. Examination of the metalation transition-state complexes reveals that $Li^{+\delta}$–$N4^{-\delta}$ electrostatic interactions yield a low energy barrier for reaction at the 5-ethyl group. Furthermore, a very stable 5-lithioethyl intermediate is formed, which markedly slows the loss back to reactant. Since N2 carries a much lower negative charge than N4, reaction at the 1-methyl group produces a significantly less stable transition-state complex and lithiated product. As a result, I1 is predicted to be formed at a much faster rate than I2. These results indicate that the only pool of reactant available for methyl–lithium exchange at the alkylation stage is the 1-methyl-5-(lithioethyl)tetrazole. According to Laidler–Eyring theory, the THF solvent reinforces the kinetic effects by selective stabilization of intermediate I1 over I2. In addition, THF acts to prevent loss of the final product by slowing reverse alkylation.

Smaller differences in barrier heights for competing reactions and in the stability of the lithiated intermediates are found in the case of the 2,5-substituted tetrazole. If all of the reactions occur with sufficient velocity, the molecule favored from considerations of equilibrium thermodynamics will be the dominant product. However, if high barriers do slow the approach to equilibrium in the alkylation step, the effects of THF on the rates of reverse

metalation will play a role in determining the outcome of the reaction. Selective solvent stabilization of the more polar 2-(lithiomethyl)-5-ethyltetrazole (**I4**) over 2-methyl-5-(lithioethyl)tetrazole (**I3**) leads to loss of **I3** back to reactant at a much higher rate than **I4**. The resultant shift in equilibrium of the metalation reaction effectively leaves **I4** as the available reactant for the alkylation step. In this case, solvation effects counter the kinetic trend calculated for a medium of unit dielectric constant and favor ultimate formation of the observed 2,5-diethyl product.